



UNIVERSITY  
OF TRENTO

---

DIPARTIMENTO DI INGEGNERIA E SCIENZA DELL'INFORMAZIONE

---

38123 Povo – Trento (Italy), Via Sommarive 14  
<http://www.disi.unitn.it>

DESIGN OF COMPROMISE SUM-DIFFERENCE PATTERNS  
THROUGH THE ITERATIVE CONTIGUOUS PARTITIONMETHOD

P. Rocca, L. Manica, A. Martini, and A. Massa

January 2009

Technical Report # DISI-11-035



# **Design of Compromise Sum-Difference Patterns through the Iterative Contiguous Partition Method**

P. Rocca, L. Manica, A. Martini, and A. Massa

Department of Information and Communication Technology,  
University of Trento, Via Sommarive 14, 38050 Trento - Italy  
Tel. +39 0461 882057, Fax +39 0461 882093

E-mail: *andrea.massa@ing.unitn.it*,

*{paolo.rocca, luca.manica, anna.martini}@dit.unitn.it*

Web-site: *http://www.eledia.ing.unitn.it*

# Design of Compromise Sum-Difference Patterns through the Iterative Contiguous Partition Method

P. Rocca, L. Manica, A. Martini, and A. Massa

## Abstract

In this paper, an innovative approach for the synthesis of sub-arrayed monopulse linear arrays is presented. A compromise difference pattern is obtained through an optimal excitations matching method based on the contiguous partition technique integrated in an iterative procedure ensuring, at the same time, the optimization of the sidelobe level (or other beam pattern features). The flexibility of such an approach allows one to synthesize various difference patterns characterized by different trade-off between angular resolution and noise/interferences rejection in order to match the user-defined requirements. On the other hand, thanks to its computational efficiency, synthesis problems concerned with large arrays are easily managed, as well. An exhaustive numerical validation assesses the reliability and accuracy of the method pointing out the improvements upon state-of-the-art sub-arraying techniques.

**Key words:** Linear Arrays, Monopulse Antennas, Sum and Difference Pattern Synthesis, Contiguous Partition.

# 1 Introduction

The design of monopulse radar systems [1][2] requires the synthesis of both a sum pattern and a difference pattern, which satisfy some specifications such as narrow beamwidth, low side-lobe-level ( $SLL$ ), and high directivity. In order to avoid an expensive implementation of independent feed networks for obtaining optimal sum [3]-[7] and difference [8]-[11] excitation coefficients, compromise solutions based on sub-arraying techniques have been successfully proposed [12]-[18]. The sum pattern is fixed to the optimal one, while difference excitations are obtained from the sum coefficients by properly grouping the array elements and by weighting each sub-array in order to satisfy the user-defined constraints. In such a context, two different methodological approaches might be recognized. The former (indicated in the following as “*optimal matching*”) is aimed at determining the “*best compromise*” difference pattern, which is as close as possible to the optimum in the Dolph-Chebyshev sense [19] (i.e., narrowest first null beamwidth and largest normalized difference slope on the boresight for a specified sidelobe level). The other, denoted as “*feature optimization*”, where the beam pattern parameters (usually, the  $SLL$  [13]-[15] or the directivity [20]) are controlled by including them in a cost function to minimize according to a global optimization stochastic procedure.

Concerning the “*optimal matching*” techniques, McNamara proposed in [12] the “*Excitation Matching*” method ( $EMM$ ) based on an expansion in terms of Zolotarev polynomials where, for each possible grouping, the corresponding sub-array coefficients are iteratively computed through pseudo-inversion of an overdetermined system of linear equations. Since such an approach does not allow the control of the beam pattern  $SLL$ , a constrained version of the method has been also introduced ([12], Sect. 5) in order to reduce the grating lobes effects and lead to sub-optimal difference patterns with a suitable compromise between  $SLL$ , beamwidth, and slope on boresight. Unfortunately, when the ratio between array elements and number of sub-arrays gets larger, the  $EMM$  is not always reliable/efficient because of the ill-conditioning of the matrix system as well as the large computational costs of the arising exhaustive evaluation process.

As far as the “*feature optimization*” class of sub-arraying methods is concerned, Ares *et al.* considered in [13] the application of a simulated annealing ( $SA$ ) algorithm for defining the

optimal sub-array weights (i.e., aimed at obtaining a difference pattern that satisfies a fixed constraint on the  $SLL$ ) starting from an assigned sub-array configuration. On the other hand, taking advantage of the problem convexity with respect to the weights of the subarrays and following the same line of the reasoning as in [21], a two-step hybrid optimization strategy has been proposed in [16][17]. By optimizing at the same time both partition functions (i.e., those functions that define the membership of the array elements to each sub-array) and the sub-array coefficients, *Lopez et al.* [14] proposed a Genetic Algorithm ( $GA$ ) based technique. In a similar fashion, a Differential Evolution ( $DE$ ) algorithm has been used in [15].

Although the optimization of elements membership and sub-array weights significantly improved the performance of sum-difference optimization methodologies, some drawbacks still remain. As a matter of fact, such techniques are usually time-consuming especially when dealing with large arrays since the dimension of the solution space significantly enlarges. Moreover, “*feature optimization*” approaches are usually formulated in terms of single-objective problems and the control of multiple features of the beam pattern (e.g.,  $SLL$ , beamwidth, difference slope on boresight) would require the use of customized and complex multi-objective strategies.

In the framework of optimal matching techniques, the present contribution is aimed at proposing a new approach for synthesizing best compromise patterns with  $SLL$  control. Towards this end, following the guidelines of the  $EMM$ , the proposed approach determines the difference solution close to the optimal Dolph-Chebyshev pattern through the search of the minimum cost-path in the non-complete binary tree of the possible aggregations by satisfying the  $SLL$  constraints through an iterative procedure (unlike global optimization methods that directly define a  $SLL$  penalty term in the cost function [13]-[15]).

The remaining of the paper is organized as follows. The problem is mathematically formulated in Section 2 where the proposed synthesis procedure is described in detail. Section 3 deals with an exhaustive numerical validation aimed at assessing the effectiveness of the proposed technique and at providing a comparison with state-of-the-art solutions. Conclusions and final remarks are drawn in Section 4.

## 2 Mathematical Formulation

Let us consider a linear uniform array of  $N = 2M$  elements and let us assume that the sum and difference patterns are obtained through a symmetric,  $\mathbf{A} = \{a_m = a_{-m}; m = 1, \dots, M\}$ , and an anti-symmetric,  $\mathbf{B} = \{b_m = -b_{-m}; m = 1, \dots, M\}$ , real excitations set, respectively. Thanks to these symmetry properties, only one half of the array elements is considered.

According to the guidelines of sub-arraying techniques, the sum pattern is obtained by fixing the sum excitations to the ideal ones,  $\mathbf{A}^{ideal} = \{\alpha_m; m = 1, \dots, M\}$  [3][4][5], while the difference excitations set is synthesized starting from the sum mode as follows

$$b_m = \sum_{q=1}^Q \alpha_m (\delta_{cmq} w_q); m = 1, \dots, M, \quad (1)$$

where  $Q$  is the number of sub-arrays,  $w_q$  is the weight associated to the  $q$ -th sub-array in the difference feed network, and  $\delta_{cmq}$  is the Kronecker delta whose value is determined according to the sub-array membership of each element of the array ( $\delta_{cmq} = 1$  if  $c_m = q$ ,  $\delta_{cmq} = 0$  otherwise,  $c_m \in [1, Q]$  being the sub-array index of the  $m$ -th array element).

In order to obtain the best compromise difference excitations (i.e., a set of excitations giving a pattern as close as possible to the ideal one in the Dolph-Chebyshev sense that satisfies at the same time a constraint on the  $SLL$ ), an innovative adaptive searching technique, indicated as *Iterative Contiguous Partition Method (ICPM)*, is applied. It consists of an inner loop aimed at ensuring the closeness of the trial solution to a “reference” ideal pattern and by an outer loop devoted at satisfying the requirements on the  $SLL$  (or another beam pattern feature).

With reference to Fig. 1, the main steps of the iterative procedure are described in the following:

- **Step 0 - Initialization.** The external iteration index is initialized ( $e = 0$ ), the optimal sum excitations  $\mathbf{A}^{ideal} = \{\alpha_m; m = 1, \dots, M\}$  are computed [3][4][5], and the user-desired sidelobe level threshold is set,  $SLL_d$ ;
- **Step 1 - Reference Difference Pattern Selection.** At the first iteration ( $e = 1$ ), an optimal - in the Dolph-Chebyshev sense - difference excitations set  $\mathbf{B}_{ref}^{(e)} = \{\beta_m^{(e)}; m = 1, \dots, M\}$  that generates a beam pattern with a sidelobe level  $SLL_{ref}^{(e)} = SLL_d$  is computed as in [8] and assumed as reference in the inner loop. Then, for each element of the array, an

identification parameter is evaluated according to one of two different strategies, namely the *Gain Sorting (GS)* algorithm

$$\left[ v_m^{(e)} \right]_{(GS)} = \frac{\beta_m^{(e)}}{\alpha_m}, \quad m = 1, \dots, M, \quad [\textit{Optimal Gain}] \quad (2)$$

or the *Residual Error Sorting (RES)* algorithm

$$\left[ v_m^{(e)} \right]_{(RES)} = \frac{\alpha_m - \beta_m^{(e)}}{\beta_m^{(e)}}, \quad m = 1, \dots, M, \quad [\textit{Optimal Residual Error}] \quad (3)$$

respectively. The identification indexes  $\{v_m^{(e)}; m = 1, \dots, M\}$  are ordered in a sorted list  $\mathbf{L} = \{l_m; m = 1, \dots, M\}$  (i.e., an ensemble where  $l_k \leq l_{k+1}$ ,  $k = 1, \dots, M - 1$ ,  $l_1 = \min_m \{v_m^{(e)}\}$ , and  $l_M = \max_m \{v_m^{(e)}\}$ );

- **Step 2 - Computation of the Compromise Solution.** With reference to the  $e$ -th target pattern, the approximation algorithm based on the *Contiguous Partition* technique is run until a suitable “*termination criterion*“ is satisfied. Accordingly, the following steps are performed:

- **Step 2.a - Solution Initialization.** The internal iteration counter is initialized [ $i(e) = 0$ ] and a starting trial grouping  $\mathbf{C}^{i(e)} = \{c_m^{i(e)}; m = 1, \dots, M\}$ , corresponding to a *Contiguous Partition*<sup>(1)</sup> of  $\mathbf{L}$  in  $Q$  subsets  $\mathbf{P}_Q^{i(e)} = \{\mathbf{L}_q^{i(e)}; q = 1, \dots, Q\}$ , is randomly generated and assumed as the optimal grouping  $\mathbf{C}_{opt}^{i(e)} = \mathbf{C}^{i(e)}$ . Successively, the sub-array weights  $\mathbf{W}^{i(e)} = \{w_q^{i(e)}; q = 1, \dots, Q\}$  are analytically computed according to

$$\left[ w_q^{i(e)} \right]_{(GS)} = \sum_{m=1}^M \delta_{c_m q} d_m \left( \mathbf{C}^{i(e)} \right), \quad q = 1, \dots, Q \quad [\textit{Estimated Gain}] \quad (4)$$

---

<sup>(1)</sup>With reference to [22], it can be easily shown that, once the parameters  $v_m^{(e)}$  have been ordered in the sorted list  $\mathbf{L} = \{l_m; m = 1, \dots, M\}$ , the grouping minimizing the cost function (7) corresponds to a *Contiguous Partition*. A grouping of array elements is a *Contiguous Partition* if the generic  $m_j$ -th array element belongs to the  $q$ -th sub-array only when two elements, namely the  $m_i$ -th element and the  $m_n$ -th one, belong to the same sub-array and the condition  $v_i^{(e)} < v_j^{(e)} < v_n^{(e)}$  holds true.

if the *GS* algorithm is adopted or

$$\left[ w_q^{i(e)} \right]_{(RES)} = \sum_{m=1}^M \frac{1}{1 + \delta_{c_m q} d_m (\mathbf{C}^{i(e)})}, \quad q = 1, \dots, Q \quad [Estimated Residual Error] \quad (5)$$

when the *RES* algorithm is used,  $d_m (\mathbf{C}^{i(e)})$  being an estimate of the identification parameter  $v_m^{(e)}$  given by

$$d_m (\mathbf{C}^{i(e)}) = \frac{\sum_{s=1}^M \alpha_s^2 \delta_{c_s c_m} v_s^{(e)}}{\sum_{s=1}^M \alpha_s^2 \delta_{c_s c_m}}, \quad m = 1, \dots, M; \quad (6)$$

- **Step 2.b - Cost Function Evaluation.** The closeness to the target pattern of the current candidate solution  $\mathbf{B}^{i(e)}$  (or in an equivalent fashion, the couple of coefficients  $\mathbf{C}^{i(e)}$  and  $\mathbf{W}^{i(e)}$ ) is quantified through the following cost function

$$\Psi \{ \mathbf{C}^{i(e)} \} = \sum_{m=1}^M \alpha_m^2 \left[ v_m^{(e)} - d_m (\mathbf{C}^{i(e)}) \right]^2. \quad (7)$$

The cost function value  $\Psi^{i(e)} = \Psi \{ \mathbf{C}^{i(e)} \}$  is compared to the best value attained up till now,  $\Psi \{ \mathbf{C}_{opt}^{i(e)-1} \} = \min_{h(e)=1, \dots, i(e)-1} [\Psi^{h(e)}]$ , and if  $\Psi \{ \mathbf{C}^{i(e)} \} < \Psi \{ \mathbf{C}_{opt}^{i(e)-1} \}$ , then the optimal trial solution is updated,  $\mathbf{B}_{opt}^{i(e)} = \mathbf{B}^{i(e)}$ ,  $\mathbf{C}_{opt}^{i(e)} = \mathbf{C}^{i(e)}$ , and  $\mathbf{W}_{opt}^{i(e)} = \mathbf{W}^{i(e)}$  as well as the optimal cost function value,  $\Psi_{opt}^{i(e)} = \Psi^{i(e)}$ ;

- **Step 2.c - Termination Criterion Check.** If a maximum number of iterations  $I$  is reached or a stationary condition  $[i(e) = I_{stat}^{(e)}]$  for the cost function value,

$$\frac{\left| K_{window} \Psi_{opt}^{i(e)-1} - \sum_{t=1}^{I_{window}} \Psi_{opt}^{t(e)} \right|}{\Psi_{opt}^{i(e)}} \leq \eta,$$

holds true ( $I_{window}$  and  $\eta$  being a fixed number of iterations and a fixed numerical threshold, respectively), then the inner loop is stopped and the following setting is assumed:  $\mathbf{C}_{opt}^{(e)} = \mathbf{C}_{opt}^{i(e)}$ ,  $\mathbf{W}_{opt}^{(e)} = \mathbf{W}_{opt}^{i(e)}$  (i.e.,  $\mathbf{B}_{opt}^{(e)} = \mathbf{B}^{i(e)}$ ), and  $\Psi_{opt}^{(e)} = \Psi_{opt}^{i(e)}$ . The procedure goes to Step 3. Otherwise, the Step 2.d is performed;

- **Step 2.d - Aggregation Updating.** The inner index is updated  $[i(e) \leftarrow i(e) + 1]$  and a new grouping vector  $\mathbf{C}^{i(e)}$  is defined. More in detail, a new contiguous

partition  $\mathbf{P}_Q^{i(e)}$  is derived from the previous one  $\mathbf{P}_Q^{i(e)-1}$  just modifying the sub-array memberships of the “*Border Elements*” defined as follows  $l_m \in \mathbf{L}_t^{i(e)} \wedge \{ (l_{m-1} \in \mathbf{L}_{t-1}^{i(e)}) \vee (l_{m+1} \in \mathbf{L}_{t+1}^{i(e)}) \}$ ,  $t \in [1; Q]$ . The corresponding sub-array weights  $\mathbf{W}^{i(e)}$  are then analytically computed as in (4) or (5). The procedure goes to Step 2.b;

- **Step 3 - Side-Lobe-Level Check.** The descriptive parameters of the beam pattern generated by the coefficients  $\mathbf{B}_{opt}^{(e)}$  are computed as well as the  $SLL$ ,  $SLL_{opt}^{(e)} = SLL \{ \mathbf{B}_{opt}^{(e)} \}$ . If  $SLL_{opt}^{(e)} \leq SLL_d$  and the “*degree of closeness*” to the reference pattern is satisfactory (e.g., some constraints on the beamwidth/directivity are satisfied), then the whole process ends and the final solution is:  $\mathbf{C}_{opt} = \mathbf{C}_{opt}^{(e)}$ ,  $\mathbf{W}_{opt} = \mathbf{W}_{opt}^{(e)}$  (i.e.,  $\mathbf{B}_{opt} = \mathbf{B}_{opt}^{(e)}$ ),  $\Psi_{opt} = \Psi_{opt}^{(e)}$ . Otherwise, the outer iteration index is updated ( $e \leftarrow e + 1$ ) and another reference pattern that satisfies the condition  $SLL_{ref}^{(e)} < SLL_{ref}^{(e-1)}$  is chosen. Then, the procedure restarts from Step 1 until  $e = E$ ,  $E$  being a fixed number of outer-loop iterations.

It is worth noting that the *Contiguous Partition* technique applied in the inner loop allows a non-negligible saving of computational resources as pointed out in Section 3 by means of some numerical experiments. As a matter of fact, according to the observation that the grouping minimizing (7) is a contiguous partition and that changing the sub-array membership of the *Border Elements* ensures to obtain another contiguous partition, it turns out that the number of possible aggregations reduces from  $U = Q^M$  (the total number of sub-array configurations) to

$$U^{(ess)} = \binom{M-1}{Q-1}. \quad (8)$$

---

<sup>(2)</sup> Dividing the ordered list  $\mathbf{L}$  into  $Q$  sub-arrays is equivalent to select  $Q - 1$  “division” points inside any of the  $M - 1$  intervals between adjacent elements.

### 3 Numerical Results

In this section, representative results from selected test cases are reported for assessing the effectiveness of the *ICPM* in providing a suitable trade-off between desired *SLL*, directivity, and beamwidth (**Sect. 3.1**) as well as in dealing with smaller (**Sect. 3.2**) and larger arrays (**Sect. 3.3**). Comparisons with state-of-the-art synthesis techniques are presented (**Sects. 3.2-3.3**), as well.

In order to quantify the optimality and accuracy of the obtained solutions, some quantitative indexes are introduced. They are expressed in terms of the angular variable  $\psi = (2\pi d/\lambda) \sin\theta$ ,  $\theta \in [0, \pi/2]$ ,  $\lambda$  and  $d$  being the free-space wavelength and the inter-element spacing, respectively. As far as the secondary lobes of the difference pattern are concerned, the “*Maximum Level of the Sidelobes*”, *SLL*, and the “*Grating Lobes Area*”

$$A_{sll} = \int_{\psi_1}^{\pi} |AF(\psi)|_n d\psi \quad (9)$$

$\psi_1$  being the angular position of the first null of the beam pattern, are evaluated. Moreover, the characteristics of the main lobe are described through the “*-3 dB Beamwidth*”,  $B_w$  [deg], and the “*Slope Area*” defined as follows

$$A_{slo} = 2 \times \left[ \max_{\psi} (|AF(\psi)|_n) \times \psi_{max} - \int_0^{\psi_{max}} |AF(\psi)|_n d\psi \right] \quad (10)$$

where  $|AF(\psi)|_n$  and  $\psi_{max}$  are the normalized array pattern and the angular position of the maximum, respectively.

Concerning the computational costs, the total number of inner iterations,  $I_{tot} = \sum_{e=1}^E I_{stat}^{(e)}$ , the CPU-time needed for reaching the final solution,  $T$ , and the total number of possible sub-array configurations,  $U$ , are analyzed.

#### 3.1 *ICPM* Performance Analysis

This section is aimed at analyzing the behavior of the iterative *SLL* control procedure in providing a suitable trade-off between *SLL*, directivity, and beamwidth. Towards this end, a linear

configuration of  $N = 2 \times M = 20$  elements with  $\lambda/2$  inter-element spacing is chosen and the sum excitations  $\mathbf{A}^{ideal}$  have been set to those of the linear Villeneuve pattern [5] with  $\bar{n} = 4$  and 25 dB sidelobe ratio. Then, for fixed values of  $Q$  ( $Q = 2, 4, 7$ ), the *ICPM* has been applied by setting the sidelobe threshold to  $SLL_d = -25$  dB and requiring a main lobe width smaller than  $B_w^{ref} = 6.0^\circ$ . The adaptive searching procedure has been carried out by considering a succession of different reference excitation sets  $\mathbf{B}_{ref}^{(e)}$ ,  $e = 1, \dots, 3$ , [19] with  $SLL_{ref}^{(1)} = -25$  dB,  $SLL_{ref}^{(2)} = -30$  dB, and  $SLL_{ref}^{(3)} = -40$  dB, respectively.

Figure 2 shows the results obtained by applying the sidelobe control procedure. As can be observed, the beam patterns synthesized by applying at each  $e$ -th iteration the *Contiguous Partition* technique show a trade-off between the angular resolution accuracy and noise rejection capabilities depending on the reference excitations  $\mathbf{B}_{ref}^{(e)}$ . As a matter of fact, when the difference main lobes get narrower, more power is wasted in the side lobes, and vice versa as confirmed by the values of the indexes reported in Tab. I. On the other hand, as expected, the *SLL* of the synthesized patterns get closer and closer to the reference one  $SLL_{ref}^{(e)}$  when  $Q$  grows (e.g.,  $SLL_{opt}^{(3)}|_{Q=2} = -16.20$  dB vs.  $SLL_{opt}^{(3)}|_{Q=7} = -31.30$  dB when  $SLL_{ref}^{(3)} = -40$  dB). Consequently, it turns out that the *ICPM* more successfully applies (i.e., satisfying the *SLL* and bandwidth requirements) when  $Q$  is not very small ( $Q > 2$ ). As a matter of fact, the iterative ( $e = 1, \dots, E$ ) procedure yields a satisfactory solution at  $e = 2$  when  $Q = 4$  (being  $SLL_{opt}^{(2)}|_{Q=4} = -22.30$  dB and  $B_w^{(2)}|_{Q=4} = 5.1622^\circ$ ) and  $Q = 7$  (being  $SLL_{opt}^{(2)}|_{Q=7} = -28.80$  dB and  $B_w^{(2)}|_{Q=7} = 5.1555^\circ$ ), while for  $Q = 2$ , whatever the iteration ( $e = 1, 2, 3$ ), the fulfillment of the *SLL* criterion is not met.

As far as the computational issues are concerned, it is worth noting that the *ICPM* allows a significant reduction of the dimension of the solution space ( $U^{(ess)}$  vs.  $U$  - Tab. I). Moreover, although the number of possible aggregations changes ( $U^{(ess)}|_{Q=2} = 9$ ,  $U^{(ess)}|_{Q=4} = 84$ , and  $U^{(ess)}|_{Q=7} = 84$ ) for different values of  $Q$ , the computational cost for reaching the termination criterion of the inner loop remains almost the same. In fact,  $I_{stat}^{(e)} = 2$  inner iterations are usually enough for determining  $\mathbf{B}_{opt}^{(e)}$ , except for the case of  $Q = 7$  when  $I_{stat}^{(1)} = 3$ .

Another interesting observation is concerned with the value of the cost function at the inner loop convergence [i.e., when  $i(e) = I_{stat}^{(e)}$ ]. For a fixed reference pattern, it monotonically

decreases as the number of sub-arrays  $Q$  tends to  $M$  (e.g.,  $\Psi_{opt}^{(1)}|_{Q=2} = 3.81 \times 10^{-1}$ ,  $\Psi_{opt}^{(1)}|_{Q=4} = 9.53 \times 10^{-2}$ , and  $\Psi_{opt}^{(1)}|_{Q=7} = 2.29 \times 10^{-3}$ ) pointing out asymptotically a more accurate matching between the sub-optimal difference mode and the reference one.

## 3.2 Comparative Assessment

In this section, a comparative analysis between the proposed approach and state-of-the-art techniques, based on the optimization of a suitable cost function constructed with reference to a  $SLL$  with a prescribed value, is carried out. Both fixed-partition (**Test Case 1**) and global-synthesis (**Test Case 2**) problems have been considered.

### Test Case 1. Fixed-Partition Synthesis

The first test case deals with the synthesis of a fixed sub-array configuration. With reference to the same benchmark in [23] and addressed by *Ares et al.* with a  $SA$ -based technique [13][23], a linear array of  $N = 2 \times M = 20$  equally-spaced ( $d = \lambda/2$ ) elements and  $Q = 3$  is considered. The optimal sum excitations have been fixed to that of a Dolph-Chebyshev pattern with  $SLL = -35$  dB and a Zolotarev difference pattern with  $SLL_{ref} = -35$  dB has been chosen as reference.

In Figure 3, the difference patterns synthesized with the  $GS$  and  $RES$  algorithms are compared with that shown in [23]. Moreover, the corresponding sub-array grouping and weights are given in Tab. II. Both the  $GS$  and  $RES$  techniques outperform the  $SA$ -based solution in terms of the maximum value the sidelobe level ( $SLL_{opt}^{(SA)} = -19.74$  dB [23] vs.  $SLL_{opt}^{(GS)} = -25.25$  dB and  $SLL_{opt}^{(RES)} = -21.31$  dB) and the gain sorting strategy allows a three fold reduction of the side lobe power (i.e.,  $\left. \frac{A_{sll}^{(SA)}}{A_{sll}^{(GS)}} \right| \simeq 3$ ). Nevertheless the solution of the  $RES$  has a  $SLL$  4 dB above that of the  $GS$ , it is worth notice that  $\left. \frac{A_{sll}^{(SA)}}{A_{sll}^{(RES)}} \right| \simeq 2$ . Moreover, by imposing the compromise patterns having a maximum  $BW$  close to that of the  $SA$ -based technique ( $B_w^{(SA)} = 5.5528^\circ$ ), the solutions from the  $GS$  and  $RES$  algorithms are shown in Fig. 3 (i.e.,  $GS^*$  and  $RES^*$  -  $SLL_{ref} = -33.75$  dB), while the corresponding sub-array configurations and weights are summarized in Tab. II. In such a situation, only the  $GS$  is able to find a better compromise pattern with a  $SLL$  below that in [23] of about 0.5 dB ( $SLL_{opt}^{(GS^*)} = -20.21$  dB -  $B_w^{(GS^*)} =$

$$5.4947^\circ; SLL_{opt}^{(RES^*)} = -19.03 \text{ dB} - B_w^{(RES^*)} = 5.3558^\circ).$$

## Test Case 2. Simultaneous Global-Synthesis

The second test case is devoted to the comparative assessment when dealing with the simultaneous optimization of the sub-array membership and sub-array weights. Towards this purpose, the proposed method is compared with the *GA*-based method [14] and the *DE* algorithm [15]. The first comparison is concerned with the *SLL* minimization of the difference pattern in a linear array of  $N = 2 \times M = 20$  elements with  $d = \lambda/2$  inter-element spacing. The optimal sum excitations have been fixed to generate a linear Villeneuve pattern [5] with  $\bar{n} = 4$  and sidelobe ratio of  $25 \text{ dB}$ . Moreover, the number of sub-arrays has been set to  $Q = 3$  for considering the same example dealt with in [14]. Concerning the *ICPM*, the reference difference pattern has been chosen to be equal to a Zolotarev pattern [19] with  $SLL_{ref} = -35 \text{ dB}$ .

The results of the synthesis process are shown in Figure 4 where the reference difference pattern and those obtained with the *GA* [14] and the constrained *EMM* [12] are displayed, as well. Concerning the comparison with the *GA*-based method, both the *GS* and *RES* schemes outperform the result in [14] ( $SLL_{opt}^{(GA)} = -26.18 \text{ dB}$ ) with a maximum side-lobe level equal to  $SLL_{opt}^{(GS)} = -28.60 \text{ dB}$  and  $SLL_{opt}^{(RES)} = -28.30 \text{ dB}$ , respectively [Tab. III], and similar bandwidths ( $B_w^{(GA)} = 5.7934^\circ$ ,  $B_w^{(GS)} = 5.8004^\circ$ , and  $B_w^{(RES)} = 5.8011^\circ$ ). It is interesting to observe that the sub-array configuration determined by both *GS* and *RES* algorithms (i.e.,  $\mathbf{C} = \{1, 2, 0, 3, 3, 3, 3, 0, 2, 1\}$ ) is the same obtained in [14], but the sub-arrays weights are different ( $\mathbf{W}^{(GA)} = \{0.3260, 0.6510, 1.2990\}$ ,  $\mathbf{W}^{(GS)} = \{0.2456, 0.6018, 1.2580\}$ , and  $\mathbf{W}^{(RES)} = \{0.2408, 0.6018, 1.2531\}$ ). Such an event is due to the fact that in [14] the sub-array gains are part of the optimization process, while in the *ICPM*-based method they are analytically computed once the sub-array configuration has been found. This allows a reduction of the number of unknowns (i.e., only the aggregations instead of weights and aggregations) and, indirectly, of the possibility the solution being trapped in local minima of the cost function. As far as the computational costs are concerned, thanks to the reduction of the number of possible aggregations ( $U^{(GA)} = 3^{10}$  vs.  $U^{(ess)} = 36$ ) and the searching limited to the sub-array membership, the number of iterations needed for reaching the final solution turns out to

be significantly lowered ( $I_{stat}^{(GS)} = I_{stat}^{(RES)} = 3$  vs.  $I_{stat}^{(GA)} = 500$  [14]) with a huge computational saving ( $T^{(ICPM)} < 0.085$  [sec]).

In order to obtain a different trade-off between sidelobe level and beamwidth, exploiting the flexibility of the proposed method, a different reference pattern could be chosen (as highlighted through the analysis in **Sect. 3.1**). As an example and for a further comparison now with another “*optimal matching*” technique instead of the *GA*, let us relax the requirement on the *SLL* and request the *BW* of the compromise patterns being as close as possible to that of the constrained *EMM* [12]. Towards this aim, a Zolotarev pattern [19] with  $SLL_{ref} = -18.87$  dB has been used as reference difference pattern. The synthesized beam patterns are shown in Figure 5. As far as the main lobe is concerned, the beamwidth of the  $GS^*$  pattern is narrower ( $B_w^{(GS^*)} = 4.5961^\circ$ ) than that of the unconstrained *GS* and very close to that by *McNamara* [12] ( $B_w^{(Const-EMM)} = 4.6090^\circ$ ). On the other hand, as expected, the performances in terms of *SLL* get worse ( $-17.25$  dB vs.  $-28.60$  dB), but they are still better than that of the *SLL*-constrained *EMM* (Tab. III). Concerning the *RES*-based method, although the trade-off solution has narrower beamwidth and higher sidelobes, it has not been possible to fit the bandwidth requirement (i.e.,  $B_w^{(RES)} > B_w^{(Const-EMM)}$  - Tab. III).

The second example addresses the same problem considered in [15][17] concerned with a 20-elements linear array with  $Q = 4$  and  $Q = 6$ , where the sum pattern is of Dolph-Chebyshev type and characterized by  $SLL = -20$  dB. By assuming reference Zolotarev patterns with  $SLL_{ref} = -30$  dB ( $Q = 4$ ) and  $SLL_{ref} = -35$  dB ( $Q = 6$ ), the optimized difference patterns are shown in Fig. 6, while the final sub-array configurations and weights are summarized in Tab. IV.

The *contiguous partition* method is more effective than both the *DE*-based approach [15] and the two-step procedure proposed in [17] (indicated in figures and tables as *Hybrid – SA* approach) in minimizing the level of the sidelobes as graphically shown in Fig. 6 and quantitatively confirmed by the behavior of the beam pattern indexes in Tab. V. Similar conclusions hold true in dealing with the required computational burden ( Tab. V) and *CPU*-time ( $T^{(GS)} < 0.2$  [sec]).

For completeness, the  $B_w$ -constrained problem has been also addressed. Accordingly, the *SLL*

minimization has been performed by requiring a beamwidth value close to that in [15] and [17] (Tab. V). The patterns computed with the sub-array configurations and weights given in Tab. IV and synthesized by means of the  $GS^*$  and  $RES^*$  algorithms ( $Q = 4 - SLL_{ref}^{Zolotarev} = -27.50 \text{ dB}$ ,  $Q = 6 - SLL_{ref}^{Zolotarev} = -33.00 \text{ dB}$ ) are shown in Fig. 6. Moreover, the corresponding pattern indexes are summarized in Tab. V.

### 3.3 Extension to Large Arrays

The numerical study ends with analysis of the synthesis of large array patterns ( $M \geq 50$ ) where usually local minima problems, unmanageable (or very difficult) increasing computational costs, and ill-conditioning issues unavoidably arise. In such a framework, the first experiment is concerned with a  $N = 2 \times M = 100$  elements array ( $d = \lambda/2$ ) with sum pattern fixed to the Taylor distribution [4] with  $\bar{n} = 12$  and  $SLL = -35 \text{ dB}$ . For comparison purposes, the case of  $Q = 4$  sub-arrays [13]-[15][17] is dealt with. Dealing with such a scenario, the  $ICPM$  has been applied by considering a reference Zolotarev pattern [19] with sidelobe level equal to  $SLL_{ref} = -40 \text{ dB}$ . In the following, only the solutions obtained with the  $GS$  are reported, since as shown in Sect. 3.2 the performance of the  $RES$  get worse when the number of array elements increases with respect to the number of sub-arrays (unavoidable for large arrays).

The synthesized difference patterns are shown in Fig. 7, while the sub-array grouping and weights are given in Tab. VI. By observing both Fig. 7 and Tab. VII, it turns out that the  $GS$  approach outperforms other single-step techniques and, unlike the case  $M = 10$ , its performances are quite similar (in terms of sidelobe level) to that of the two-step method even though it is much more computationally effective. Moreover, although it achieves the minimum value of  $SLL$ , the corresponding main lobe beamwidth does not significantly differ from that of the other methods (Tab. VII).

In the second experiment, the same array geometry of the previous case is analyzed, but with  $Q = 3$  sub-arrays analogous to [14]. The sub-array configuration and weights obtained with the  $GS$ -based strategy are reported in Tab. VIII. Also in this case, the  $GS$  difference pattern presents a  $SLL$  lower than that shown in [14] ( $SLL_{opt}^{(GS)} = -30.25$  vs.  $SLL_{opt}^{(GA)} = -29.50$ ) and confirms its effectiveness in terms of computational resource since  $\frac{I_{stat}^{(GA)}}{I_{stat}^{(GS)}} = 250$ .

Finally, the last experiment is concerned with a very large array of  $N = 200$  elements ( $d = \lambda/2$ ). In such a case, the sum pattern excitations have been chosen to produce a Dolph-Chebyshev pattern [3] with  $SLL = -25$  dB, while reference difference excitations able to generate a Zolotarev pattern [19] with  $SLL_{ref} = -30$  dB have been assumed. Moreover, the number of sub-arrays has been set  $Q = 6$ .

The beam pattern synthesized with the  $GS$  algorithm is shown in Fig. 8. As it can be noticed, although the ratio between the number of elements and the number of sub-arrays is not negligible ( $\frac{M}{Q} \simeq 17$ ), the obtained solution ensures a  $SLL_{opt}^{(GS)} = -25.15$  dB assessing the reliability of the proposed method in dealing with large structures, unlike the  $EMM$ , which suffers in this framework from the severe ill-conditioning of the matrix system.

## 4 Conclusions and Discussions

In this paper, an innovative approach for the synthesis of search-and-track antennas and beam patterns for monopulse radar applications has been presented. The proposed method consists of an adaptive searching procedure whose result is a compromise solution as close as possible to an optimal one in the Dolph-Chebyshev sense, which allows a satisfactory trade-off between angular resolution and reduction of noise and interferences effects. In particular, the narrowest beamwidth and the largest slope around the boresight direction are looked for by applying the optimal excitation matching method based on the contiguous partition technique, while the fulfillment of the requirements on the  $SLL$  (or other beam pattern features) is ensured by an outer iterative loop.

The obtained results have proved the effectiveness of the proposed approach in providing difference patterns with a satisfactory trade-off among beam pattern features dealing with large arrays, as well. Although the iterative contiguous partition method is aimed at synthesizing the “best compromise” matching an optimal (in the Dolph-Chebyshev sense) reference pattern, the obtained solutions positively compare with state-of-the-art approaches in the related literature in a number of measures where only the  $SLL$  minimization is required, thus showing how the proposed approach, which is numerically efficient, works sufficiently well. As a matter of fact, the proposed technique allows one to overcome some drawbacks of both the  $EMM$  approach

proposed by *McNamara* (i.e., ill-conditioning and the exhaustive evaluation of the whole set of aggregations) and the synthesis techniques based on stochastic optimization algorithms (i.e., single-objective optimization and low convergence rate when dealing with very large arrays). For the sake of completeness and to have a complete overview of the comparisons between the proposed method and the state-of-the-art techniques, Tables IX and X summarize the achieved performance in terms of  $SLL$  and  $B_w$  when dealing with the synthesis of small and large arrays. On the other hand, definite conclusions about the relative performance of the *ICPM* cannot be drawn from the presented comparisons, since the various examples deal with different synthesis problems and/or optimization criteria. This means that, depending on the selected feature, the *ICPM* performs differently even though keeping a great computational efficiency. Moreover, since the proposed procedure is an adaptive searching technique, it does not guarantee to always obtain better solutions than those from global optimization techniques. As a matter of fact, these latter should outperform any other approach when optimizing a given functional, unless the optimum is not actually achieved, which is likely to happen when exploiting global optimization algorithms in large size problems.

## Acknowledgments

The authors wish to thank Prof. T. Isernia and Dr. M. Donelli for useful discussions. Moreover, the authors are indebted to the anonymous reviewers for their constructive comments, which significantly improved this paper. This work has been partially supported in Italy by the “*Progettazione di un Livello Fisico 'Intelligente' per Reti Mobili ad Elevata Riconfigurabilità*,” Progetto di Ricerca di Interesse Nazionale - MIUR Project COFIN 2005099984.

## References

- [1] Skolnik, M.I.: 'Introduction of Radar System' (McGraw-Hill, 3rd edn., 2001)
- [2] Wirth, W.: 'Radar Techniques using Array Antennas' (IET Press, 2001)

- [3] Dolph, C.L.: 'A current distribution for broadside arrays which optimises the relationship between beam width and sidelobe level', *IRE Proc.*, 1946, (34), pp. 335-348
- [4] Taylor, T.T.: 'Design of line-source antennas for narrow beam-width and low side lobes', *IRE Trans. Antennas Propagat.*, 1955, (3), pp. 16-28
- [5] Villeneuve, A.T.: 'Taylor patterns for discrete arrays', *IEEE Trans. Antennas Propagat.*, 1984, AP-32, pp. 1089-1093
- [6] Isernia, T., Di Iorio, P., and Soldovieri, F.: 'An effective approach for the optimal focusing of array fields subject to arbitrary upper bounds', *IEEE Trans. Antennas Propagat.*, 2000, 48, pp. 1837-1847
- [7] Bucci, O.M., Caccavale, L., and Isernia, T.: 'Optimal far-field focusing of uniformly spaced arrays subject to arbitrary upper bounds in nontarget directions', *IEEE Trans. Antennas Propagat.*, 2002, 50, pp. 1539-1554
- [8] McNamara, D.A.: 'Discrete  $\bar{n}$ -distributions for difference patterns', *Electron. Lett.*, 1986, 22, (6), pp. 303-304
- [9] McNamara, D.A.: 'Performance of Zolotarev and modified-Zolotarev difference pattern array distributions', *IEE Proc. Microwave Antennas Propagat.*, 1994, 141, (1), pp. 37-44
- [10] Willis, A.J., and Baker, C.J.: 'Approximation to Zolotarev polynomial ideal difference beams for linear arrays', *Electron. Lett.*, 2006, 42, (10), pp. 561-563
- [11] Bucci, O.M., D'Urso, M., and Isernia, T.: 'Optimal synthesis of difference patterns subject to arbitrary sidelobe bounds by using arbitrary array antennas', *IEE Proc. Microwave Antennas Propagat.*, 2005, 152, pp. 129-137
- [12] McNamara, D.A.: 'Synthesis of sub-arrayed monopulse linear arrays through matching of independently optimum sum and difference excitations', *IEE Proc. H*, 1988, 135, (5), pp. 371-374

- [13] Ares, F., Rengarajan, S.R., Rodriguez J.A., and Moreno, E.: 'Optimal compromise among sum and difference patterns through sub-arraying', *Proc. IEEE. Antennas Propagat. Symp.*, Baltimore, USA, July 1996, pp. 1142-1145
- [14] Lopez, P., Rodriguez, J.A., Ares, F., and Moreno, E.: 'Subarray weighting for difference patterns of monopulse antennas: joint optimization of subarray configurations and weights', *IEEE Trans. Antennas Propagat.*, 2001, 49, (11), pp. 1606-1608
- [15] Caorsi, S., Massa, A., Pastorino, M., and Randazzo, A.: 'Optimization of the difference patterns for monopulse antennas by a hybrid real/integer-coded differential evolution method', *IEEE Trans. Antennas Propagat.*, 2005, 53, (1), pp. 372-376
- [16] D'Urso, M., and Isernia, T.: 'Solving some array synthesis problems by means of an effective hybrid approach', *IEEE Trans. Antennas Propagat.*, 2007, 55, (3), pp. 750-759
- [17] D'Urso, M., Isernia, T., and Meliadó, E.F.: 'An effective hybrid approach for the optimal synthesis of monopulse antennas', *IEEE Trans. Antennas Propagat.*, 2007, 55, (4), pp. 1059-1066
- [18] Fondevila, J., Brégains, J.C., Ares, F., and Moreno E.: 'Application of the time modulation in the synthesis of sum and difference patterns by using linear arrays', *Microwave Optical Technol. Lett.*, 2006, 48, (5), pp. 829-832
- [19] McNamara, D.A.: 'Direct synthesis of optimum difference patterns for discrete linear arrays using Zolotarev distribution', *IEE Proc. H*, 1993, 140, (6), pp. 445-450
- [20] Massa, A., Pastorino, M., and Randazzo, A.: 'Optimization of the directivity of a monopulse antenna with a subarray weighting by a hybrid differential evolution method', *IEEE Antennas Wireless Propagat. Lett.*, 2006, 5, (1), pp. 155-158
- [21] Isernia, T., Ares-Pena, F., Bucci, O.M., D'Urso, M., Gomez, X.F., and Rodriguez, A.: 'A hybrid approach for the optimal synthesis of pencil beams through array antennas', *IEEE Trans. Antennas Propagat.*, 2004, pp. 2912-2918

- [22] Fisher, W.D.: 'On grouping for maximum homogeneity', *American Statistical Journal*, 1958, pp. 789-798
- [23] Ares, F., Rodriguez, J.A., Moreno, E., and Rengarajan, S.R.: 'Optimal compromise among sum and difference patterns', *J. Electromagn. Waves Applicat.*, 1996, 10, (11), pp. 1543-1555
- [24] Rocca, P., Manica, L. , and Massa, A.: 'Synthesis of monopulse antennas through iterative contiguous partition method,' , *Electron. Lett.*, 2007, 43, (16), pp. 854-856

## FIGURE CAPTIONS

- **Figure 1.** Flow chart of the *Iterative Contiguous Partition Method*.
- **Figure 2.** *ICPM Performance Analysis* ( $M = 10, d = \frac{\lambda}{2}$ ) - Normalized difference patterns when (a)  $Q = 2$  , (b)  $Q = 4$ , and (c)  $Q = 7$ .
- **Figure 3.** *Comparative Assessment* ( $M = 10, d = \frac{\lambda}{2}, Q = 3$ ) - Normalized difference patterns synthesized with the *ICPM – GS*, the *ICPM – RES*, and the *SA* algorithm [23].
- **Figure 4.** *Comparative Assessment* ( $M = 10, d = \frac{\lambda}{2}, Q = 3$ ) - Reference pattern ( $SLL_{ref} = -35 \text{ dB}$ ) and normalized difference patterns synthesized with the *ICPM – GS*, the *ICPM – RES*, the *GA*-based method [14], and the constrained *EMM* [12].
- **Figure 5.** *Comparative Assessment* ( $M = 10, d = \frac{\lambda}{2}, Q = 3$ ) - Normalized difference patterns synthesized with the *ICPM – GS*, the *ICPM – RES*, the *GA*-based method [14], and the constrained *EMM* [12].
- **Figure 6.** *Comparative Assessment* ( $M = 10, d = \frac{\lambda}{2}$ ) - Normalized difference patterns synthesized with the *ICPM – GS*, the *ICPM – RES*, the *Hybrid – SA* approach [17], and the *DE* algorithm [15] when (a)  $Q = 4$  and (b)  $Q = 6$ .

- **Figure 7.** *Extension to Large Arrays* ( $M = 50, d = \frac{\lambda}{2}, Q = 4$ ) - Normalized difference patterns synthesized with the *ICPM – GS* ( $SLL_{ref} = -40$  dB), the *SA* algorithm [23], the *Hybrid – SA* approach [17], the *GA*-based method [14], and the *DE* algorithm [15].
- **Figure 8.** *Extension to Large Arrays* ( $M = 100, d = \frac{\lambda}{2}, Q = 6$ ) - Normalized difference patterns synthesized with the *ICPM – GS* ( $SLL_{ref} = -30$  dB).

## TABLE CAPTIONS

- **Table I.** *ICPM Performance Analysis* ( $M = 10, d = \frac{\lambda}{2}$ ) - Difference pattern quantitative indexes and computational indicators for different values of  $Q$ .
- **Table II.** *Comparative Assessment* ( $M = 10, d = \frac{\lambda}{2}, Q = 3, SLL_{ref} = -35$  dB) - Sub-array configuration and weights synthesized with the *ICPM – GS* and the *ICPM – RES*.
- **Table III.** *Comparative Assessment* ( $M = 10, d = \frac{\lambda}{2}, Q = 3$ ) - Quantitative indexes of the reference pattern ( $SLL_{ref} = -35$  dB) and of the difference patterns synthesized with the *ICPM – GS*, the *ICPM – RES*, the *GA*-based method [14], and the constrained *EMM* [12].
- **Table IV.** *Comparative Assessment* ( $M = 10, d = \frac{\lambda}{2}$ ) - Sub-array configuration and weights synthesized with the *ICPM – GS* and the *ICPM – RES*, when  $Q = 4$  and  $Q = 6$ .
- **Table V.** *Comparative Assessment* ( $M = 10, d = \frac{\lambda}{2}$ ) - Quantitative indexes and computational indicators for the solutions obtained with the *ICPM – GS*, the *ICPM – RES*, the *Hybrid – SA*<sup>(3)</sup> approach [17], and the *DE* algorithm [15] when  $Q = 4$  and  $Q = 6$ .
- **Table VI.** *Extension to Large Arrays* ( $M = 50, d = \frac{\lambda}{2}, Q = 4$ ) - Sub-array configuration and weights synthesized with the *ICPM – GS*.

---

<sup>(3)</sup>  $I_{stat} = 25$  indicates the number of *SA* iterations (i.e., first step), no indications on the convex programming procedure (i.e., second step) are available.

- **Table VII.** *Extension to Large Arrays* ( $M = 50, d = \frac{\lambda}{2}, Q = 4$ ) - Quantitative indexes and computational indicators for the solutions obtained with the *ICPM-GS* ( $SLL_{ref} = -40$  dB), the *Hybrid-SA*<sup>(3)</sup>, the *SA* algorithm [23], the *GA*-based method [14], and the *DE* algorithm [15].
- **Table VIII.** *Extension to Large Arrays* ( $M = 50, d = \frac{\lambda}{2}, Q = 3$ ) - Sub-array configuration and weights synthesized with the *ICPM-GS*.
- **Table IX.** *Resume* ( $M = 10, d = \frac{\lambda}{2}$ ) - Quantitative indexes for the solutions obtained with the *ICPM* based approaches and state of the art techniques.
- **Table X.** *Resume* ( $M = 50, d = \frac{\lambda}{2}$ ) - Quantitative indexes for the solutions obtained with the *ICPM* based approaches and state of the art techniques.

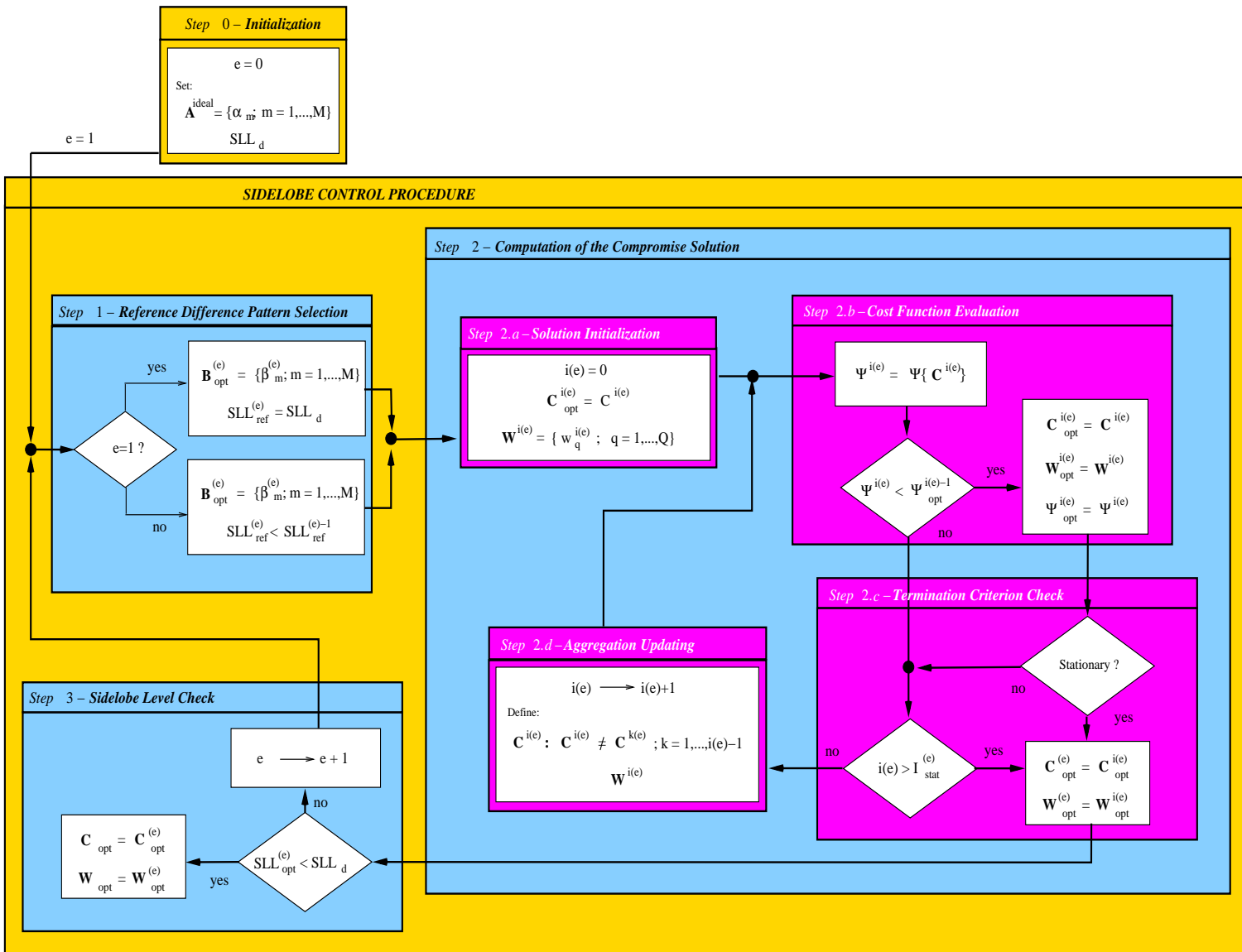
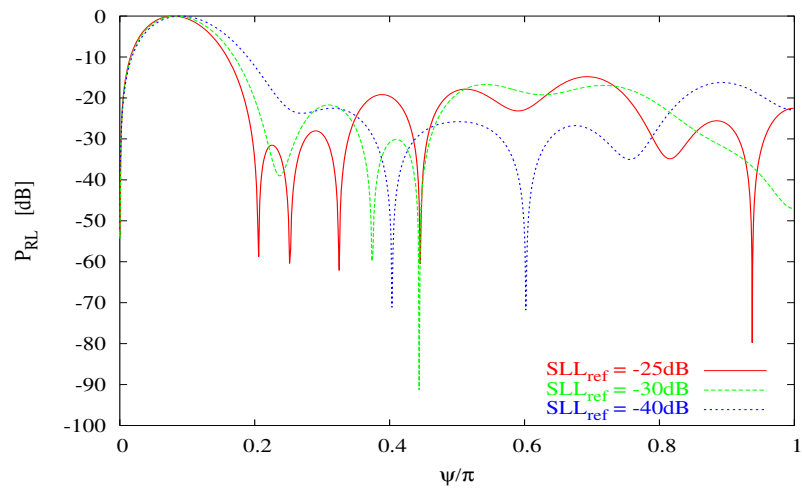
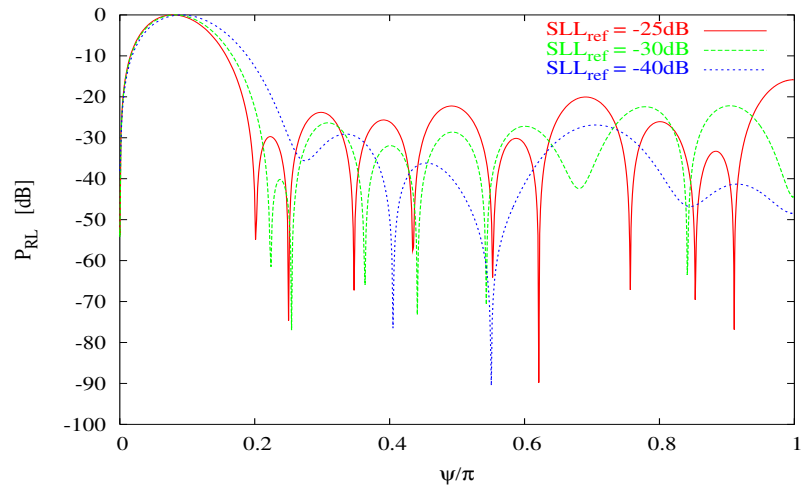


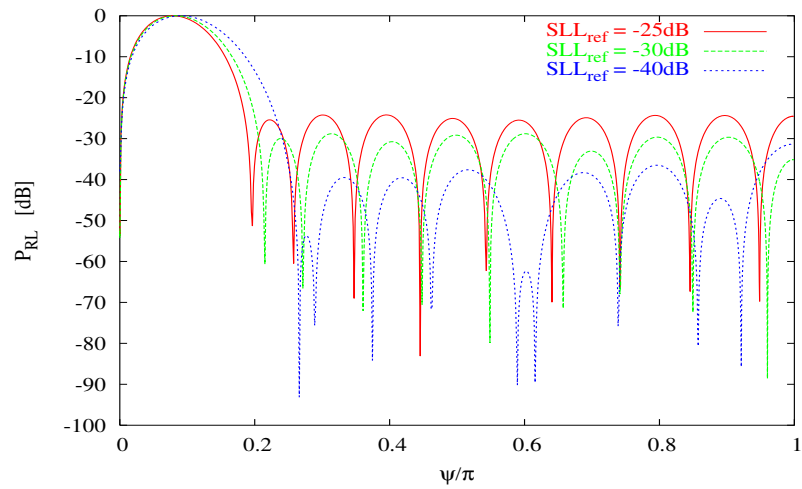
Fig. 1 - P. Rocca et al., "Compromise sum-difference optimization ..."



(a)



(b)



(c)

Fig. 2 - P. Rocca *et al.*, “Compromise sum-difference optimization ...”

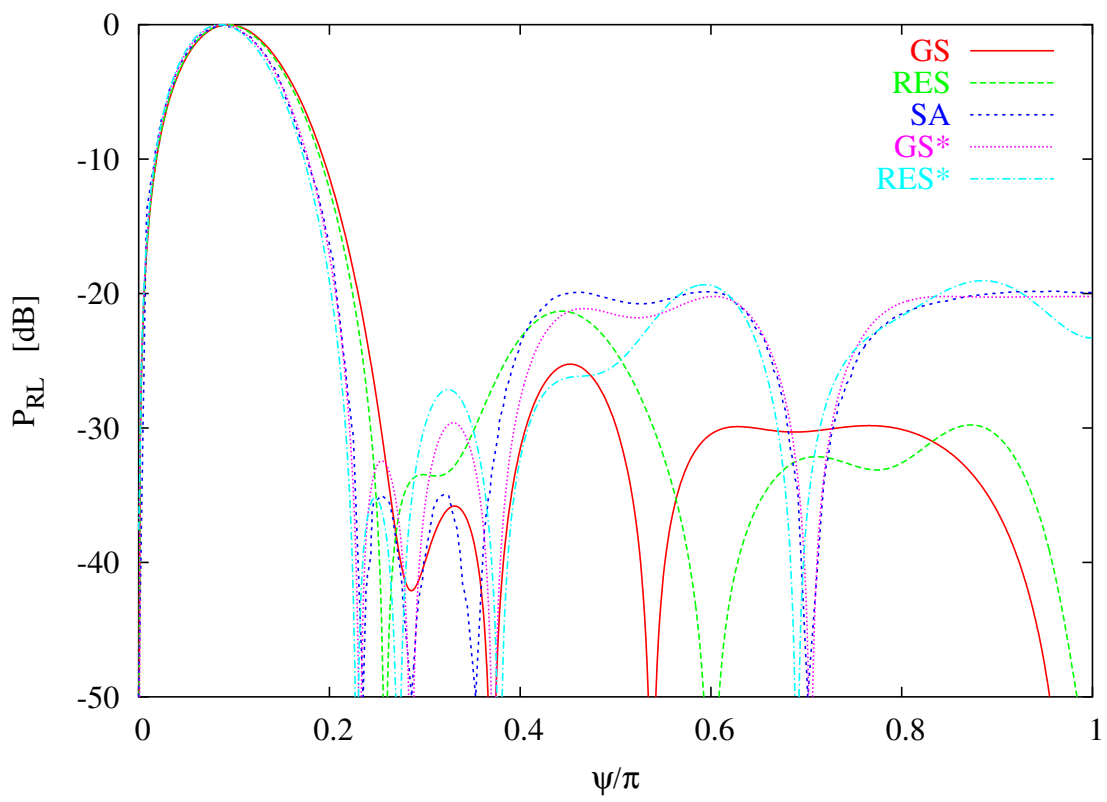


**Fig. 3 - P. Rocca *et al.*, “Compromise sum-difference optimization ...”**

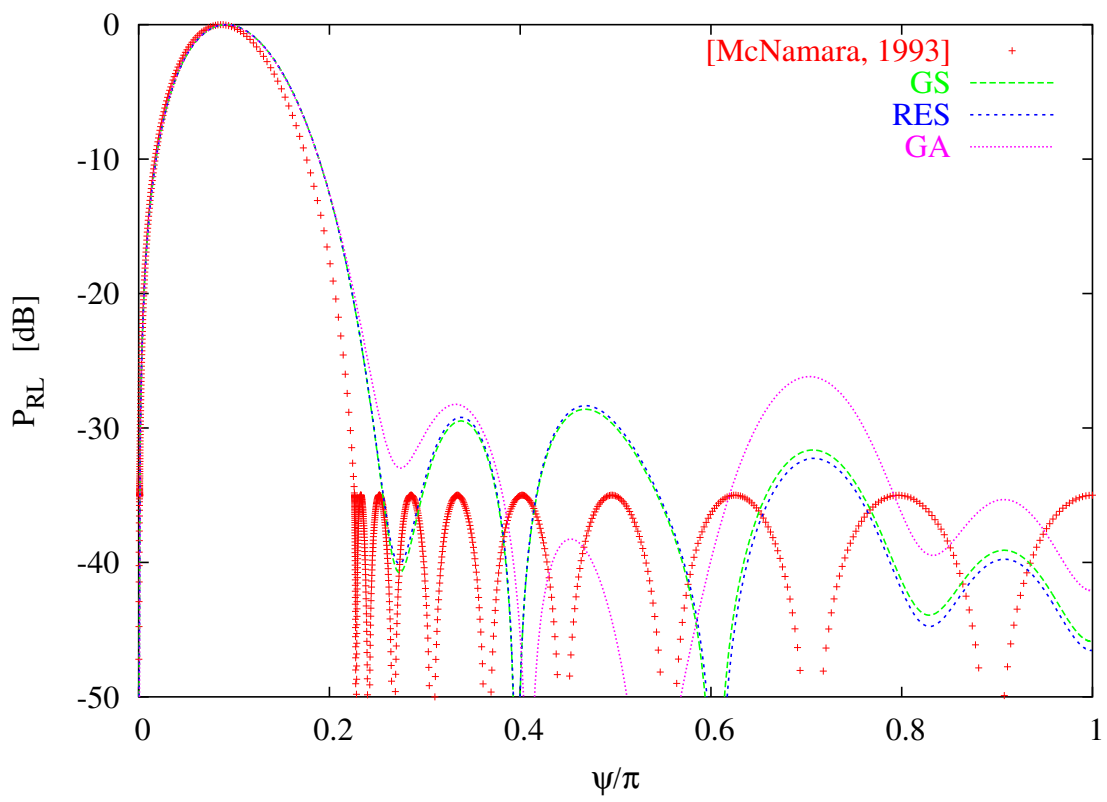
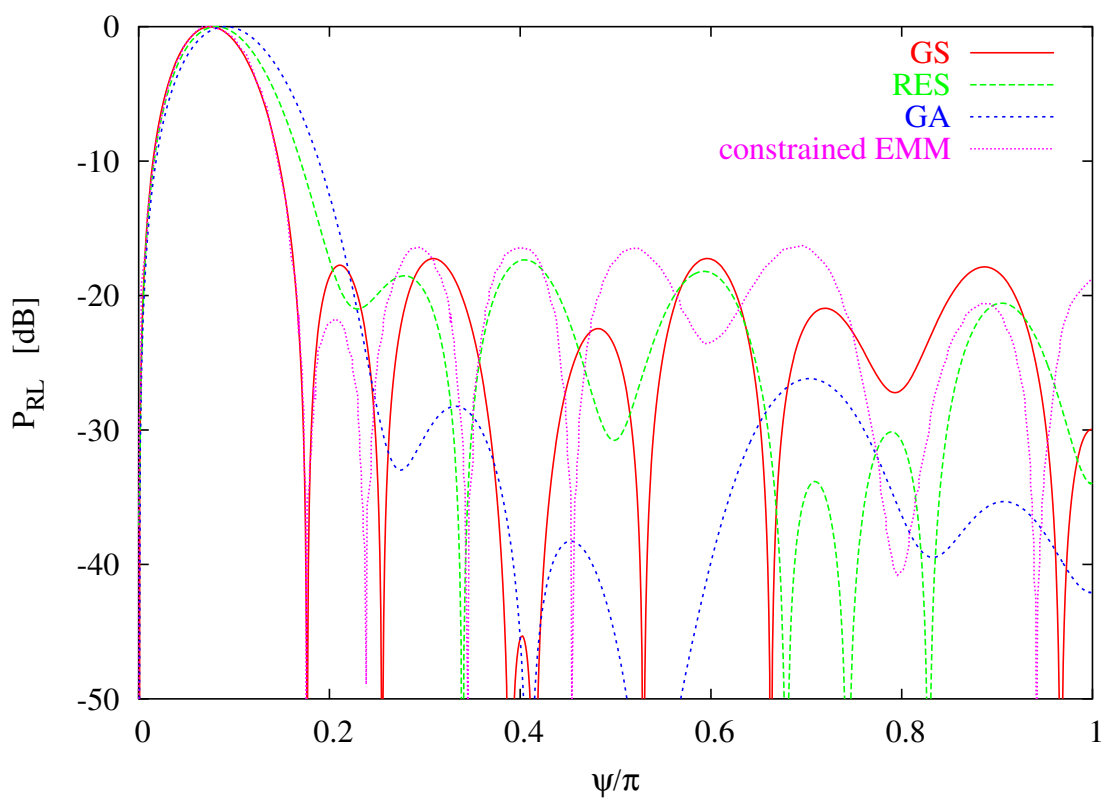


Fig. 4 - P. Rocca *et al.*, “Compromise sum-difference optimization ...”



**Fig. 5 - P. Rocca *et al.*, “Compromise sum-difference optimization ...”**

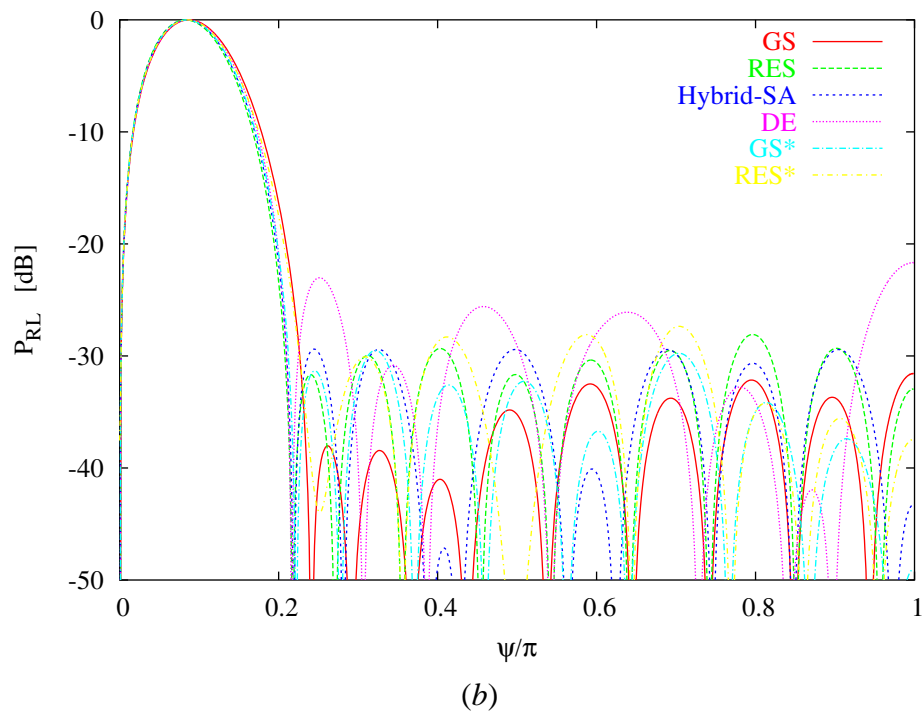
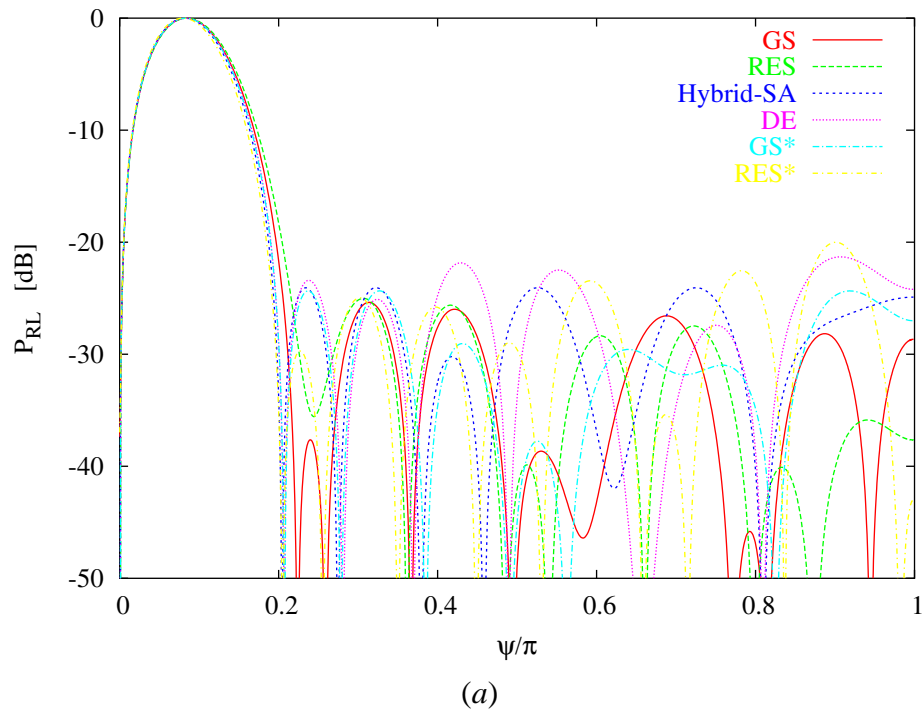
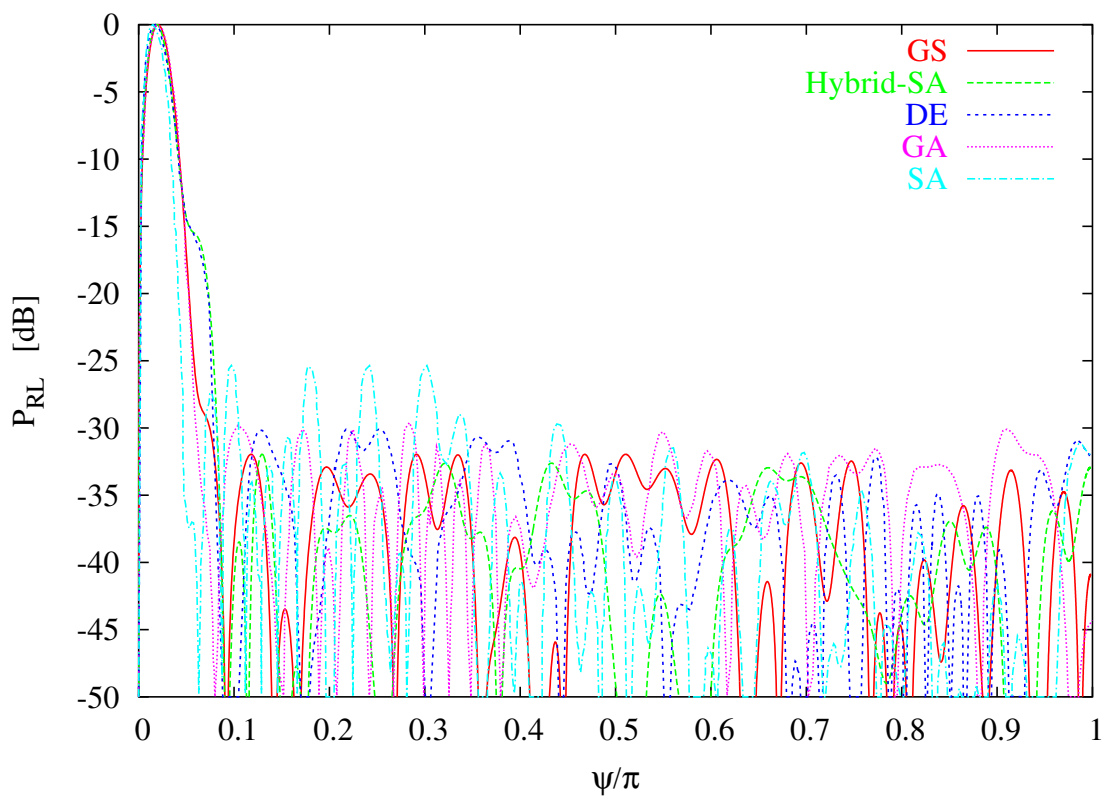
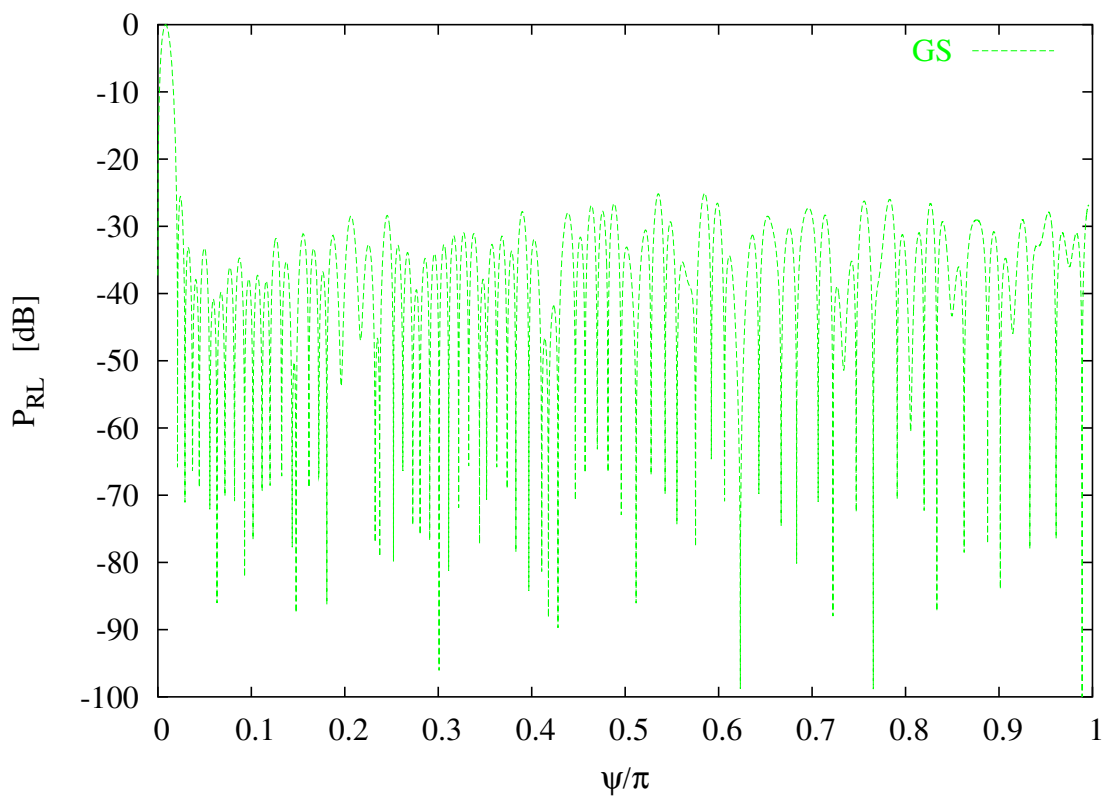


Fig. 6 - P. Rocca *et al.*, “Compromise sum-difference optimization ...”



**Fig. 7 - P. Rocca *et al.*, “Compromise sum-difference optimization ...”**



**Fig. 8 - P. Rocca *et al.*, “Compromise sum-difference optimization ...”**

Tab. I - P. Rocca *et al.*, ‘‘Compromise sum-difference optimization ...’’

	$Q = 2$			$Q = 4$			$Q = 7$		
$e$	1	2	3	1	2	3	1	2	3
$SLL_{ref}^{(e)}$	$-25\text{ dB}$	$-30\text{ dB}$	$-40\text{ dB}$	$-25\text{ dB}$	$-30\text{ dB}$	$-40\text{ dB}$	$-25\text{ dB}$	$-30\text{ dB}$	$-40\text{ dB}$
$A_{slo}$	0.1773	0.1865	0.1953	0.1759	0.1840	0.1981	0.1753	0.1844	0.1955
$B_w$ [deg]	4.9239	5.2356	5.7661	4.8910	5.1622	5.7976	4.8547	5.1555	5.7217
$\psi_1$	0.6458	0.7474	0.8463	0.6226	0.7043	0.8653	0.6197	0.6753	0.8368
$A_{sll}$	0.1761	0.1722	0.1333	0.1112	0.0780	0.0375	0.0938	0.0495	0.0179
$SLL_{opt}^{(e)}$	$-14.80$	$-16.70$	$-16.20$	$-15.80$	$-22.30$	$-26.90$	$-24.35$	$-28.80$	$-31.30$
$I_{stat}^{(e)}$	2	2	2	2	2	2	3	2	2
$\Psi_{opt}^{(e)}$	$3.81 \times 10^{-1}$	$4.62 \times 10^{-1}$	$2.76 \times 10^{-1}$	$9.53 \times 10^{-2}$	$1.10 \times 10^{-1}$	$3.89 \times 10^{-2}$	$2.29 \times 10^{-3}$	$9.93 \times 10^{-4}$	$5.45 \times 10^{-3}$
$U^{(ess)}$	9			84			84		
$U$	1024			1048580			$2.8247 \times 10^8$		

$M = 10$	$\mathbf{C}_{opt}^{(GS)} = \mathbf{C}_{opt}^{(RES)}$	1 1 2 2 2 3 3 3 3 0		
$Q = 3$	$\mathbf{W}_{opt}^{(GS)}$	0.2804	0.5839	1.3971
	$\mathbf{W}_{opt}^{(RES)}$	0.1943	0.4505	1.3897
$Q = 3$	$\mathbf{W}_{opt}^{(GS^*)}$	0.4618	2.1607	2.9448
	$\mathbf{W}_{opt}^{(RES^*)}$	0.2833	1.1443	1.3971

**Tab. II - P. Rocca *et al.*, “Compromise sum-difference optimization ...”**

	$A_{slo}$	$B_w$ [deg]	$A_{sll}$	$SLL$
<i>Reference Difference</i> [19]	0.1933	5.7668	0.0273	-35.00
<i>GS</i>	0.2046	5.8004	0.0382	-28.60
<i>RES</i>	0.2046	5.8011	0.0378	-28.30
<i>Reference Difference*</i> [19]	0.1645	4.4747	0.1526	-18.87
<i>GS*</i>	0.1690	4.5961	0.1453	-17.25
<i>RES*</i>	0.1759	5.1615	0.1530	-17.34
<i>GA Optimization</i> [14]	0.2038	5.7934	0.0440	-26.18
<i>Constrained EMM</i> [12]	0.1715	4.6090	0.2223	-16.50

**Tab. III - P. Rocca *et al.*, “Compromise sum-difference optimization ...”**

$M = 10$	$\mathbf{C}_{opt}^{(GS)}$	1 2 3 4 4 4 4 3 1							
	$\mathbf{C}_{opt}^{(RES)}$	1 2 3 4 4 4 4 3 3 1							
	$\mathbf{C}_{opt}^{(GS^*)}$	1 2 3 3 4 4 4 4 3 1							
	$\mathbf{C}_{opt}^{(RES^*)}$	1 2 3 3 4 4 4 4 3 2							
$Q = 4$	$\mathbf{W}_{opt}^{(GS)}$	0.2201	0.4601	0.6932	0.9568				
	$\mathbf{W}_{opt}^{(RES)}$	0.1837	0.4549	0.7423	0.9080				
	$\mathbf{W}_{opt}^{(GS^*)}$	0.3593	0.7882	1.5351	2.0122				
	$\mathbf{W}_{opt}^{(RES^*)}$	0.1564	0.3851	0.7732	1.0104				
$M = 10$	$\mathbf{C}_{opt}^{(GS)}$	1 2 3 4 5 6 4 3 2 1							
	$\mathbf{C}_{opt}^{(RES)}$	1 3 4 5 6 6 6 5 4 2							
	$\mathbf{C}_{opt}^{(GS^*)}$	1 2 3 5 6 6 6 4 3 1							
	$\mathbf{C}_{opt}^{(RES^*)}$	1 3 5 6 6 6 6 5 4 2							
$Q = 6$	$\mathbf{W}_{opt}^{(GS)}$	0.1714	0.5075	0.7332	0.9083	0.9901	0.9926		
	$\mathbf{W}_{opt}^{(RES)}$	0.1632	0.2613	0.4606	0.7021	0.8831	1.0049		
	$\mathbf{W}_{opt}^{(GS^*)}$	0.1876	0.4765	0.6894	0.8189	0.8914	0.9857		
	$\mathbf{W}_{opt}^{(RES^*)}$	0.1685	0.2024	0.4765	0.6321	0.7576	0.9579		

**Tab. IV - P. Rocca et al., "Compromise sum-difference optimization ..."**

	$A_{slo}$	$B_w$ [deg]	$A_{sll}$	$SLL$	$U$	$I_{stat}$
$Q = 4$						
<i>Reference Difference</i> [19]	0.1786	5.1496	0.0510	-30.00	-	-
<i>GS</i>	0.1809	5.2247	0.0564	-25.40	84	2
<i>RES</i>	0.1894	5.3228	0.0537	-25.01	84	2
<i>Reference Difference*</i> [19]	0.1803	5.0000	0.0694	-27.50	-	-
<i>GS*</i>	0.1863	5.1449	0.0748	-24.30	84	2
<i>RES*</i>	0.1742	4.9585	0.0936	-20.00	84	1
<i>Hybrid – SA</i> [17]	0.1844	5.1442	0.0919	-24.10	$\mathcal{O}(10^3)$	25
<i>DE Algorithm</i> [15]	0.1878	5.1834	0.1107	-21.30	$\mathcal{O}(10^3)$	9
$Q = 6$						
<i>Reference Difference</i> [19]	0.1929	5.4188	0.0281	-35.00	-	-
<i>GS</i>	0.1948	5.4928	0.0291	-31.56	126	2
<i>RES</i>	0.1855	5.1728	0.0500	-28.09	126	2
<i>Reference Difference*</i> [19]	0.1897	5.3138	0.0355	-33.00	-	-
<i>GS*</i>	0.1893	5.2694	0.0356	-29.52	126	2
<i>RES*</i>	0.1848	5.3827	0.0446	-27.35	126	2
<i>Hybrid – SA</i> [17]	0.1884	5.2615	0.0439	-29.50	$\mathcal{O}(10^5)$	25
<i>DE Algorithm</i> [15]	0.1942	5.3872	0.0727	-21.66	$\mathcal{O}(10^5)$	7

Tab. V - P. Rocca et al., “Compromise sum-difference optimization ...”



Tab. VII - P. Rocca *et al.*, “Compromise sum-difference optimization ...”

<i>Synthesis Approach</i>	$SLL_{opt}$	$A_{sll}$	$B_w$ [deg]	$A_{slo}$	$U$	$I_{stat}$	$T$ [sec]
<i>SA Optimization</i> [13]	-25.56	0.0432	1.0745	0.0329	$\mathcal{O}(10^{30})$	—	—
<i>GA Optimization</i> [14]	-31.00	0.0504	1.3585	0.0529	$\mathcal{O}(10^{30})$	500	$\sim 15$
<i>DE Algorithm</i> [15]	-30.00	0.0361	1.3256	0.0361	$\mathcal{O}(10^{30})$	804	$\sim 20$
<i>Hybrid – SA Method</i> [17]	-32.00	0.0305	1.2776	0.0401	$\mathcal{O}(10^{30})$	25	—
<i>GS</i>	-32.10	0.0363	1.2952	0.0444	18424	5	1.0785

$M = 50$	$\mathbf{C}_{opt}^{(GS)}$	11111222202000333333333333330330000222222211111111		
$Q = 3$	$\mathbf{W}_{opt}^{(GS)}$	0.2437	0.7079	1.0976

**Tab. VIII - P. Rocca et al., “Compromise sum-difference optimization ...”**

$M$	$Q$	<i>Synthesis Approach</i>	$SLL_{opt}$ [dB]	$B_w$ [deg]	<i>Fig. #</i>	<i>Tab. #</i>
10	3	<i>SA</i> [13]	-19.74	5.5528	3	-
		<i>ICPM – GS*</i>	-20.21	5.4947	3	-
		<i>ICPM – RES*</i>	-19.03	5.3558	3	-
10	3	<i>GA</i> [14]	-26.18	5.7934	4	<i>III</i>
		<i>ICPM – GS</i>	-28.60	5.8004	4	<i>III</i>
		<i>ICPM – RES</i>	-28.30	5.8011	4	<i>III</i>
10	3	<i>Constrained EMM</i> [12]	-16.50	4.6090	5	<i>III</i>
		<i>ICPM – GS*</i>	-17.25	4.5961	5	<i>III</i>
		<i>ICPM – RES*</i>	-17.34	5.1615	5	<i>III</i>
10	4	<i>DE</i> [15]	-21.30	5.1834	6(a)	<i>V</i>
		<i>Hybrid – SA</i> [17]	-24.10	5.1442	6(a)	<i>V</i>
		<i>ICPM – GS*</i>	-24.30	5.1449	6(a)	<i>V</i>
		<i>ICPM – RES*</i>	-20.00	4.9585	6(a)	<i>V</i>
10	6	<i>DE</i> [15]	-21.66	5.3872	6(b)	<i>V</i>
		<i>Hybrid – SA</i> [17]	-29.50	5.2615	6(b)	<i>V</i>
		<i>ICPM – GS*</i>	-29.52	5.2694	6(b)	<i>V</i>
		<i>ICPM – RES*</i>	-27.35	5.3827	6(b)	<i>V</i>
10	8	<i>DE</i> [15]	-21.59	6.3820	3 [24]	<i>I</i> [24]
		<i>Hybrid – SA</i> [17]	-36.50	5.8202	3 [24]	<i>I</i> [24]
		<i>ICPM – GS</i>	-40.85	5.8605	3 [24]	<i>I</i> [24]

**Tab. IX - P. Rocca *et al.*, “Compromise sum-difference optimization ...”**

$M$	$Q$	<i>Synthesis Approach</i>	$SLL_{opt}$ [dB]	$B_w$ [deg]	<i>Fig. #</i>	<i>Tab. #</i>
50	3	<i>GA</i> [14]	-29.50	1.2753	—	—
		<i>ICPM – GS</i>	-30.25	1.2880	—	—
50	4	<i>SA</i> [13]	-25.56	1.0745	7	<i>VII</i>
		<i>GA</i> [14]	-31.00	1.3585	7	<i>VII</i>
		<i>DE</i> [15]	-30.00	1.3256	7	<i>VII</i>
		<i>Hybrid – SA</i> [17]	-32.00	1.2776	7	<i>VII</i>
		<i>ICPM – GS</i>	-32.10	1.2952	7	<i>VII</i>

**Tab. X - P. Rocca *et al.*, “Compromise sum-difference optimization ...”**